



Published in final edited form as:

Nat Biotechnol. 2011 February ; 29(2): 158–163. doi:10.1038/nbt.1742.

Efficient Mucosal Delivery of Vaccine Using the FcRn-Mediated IgG Transfer Pathway

Lilin Ye[†], Rongyu Zeng[†], Yu Bai[†], Derry C. Roopenian[‡], and Xiaoping Zhu^{†,*},²

[†]Laboratory of Immunology, Virginia-Maryland College of Veterinary Medicine, University of Maryland, College Park, MD 20742, USA

^{*}Maryland Pathogen Research Institute, University of Maryland, College Park, MD 20742, USA

[‡]The Jackson Laboratory, 600 Main Street, Bar Harbor, ME 04609, USA

Abstract

Vaccine strategies to prevent invasive mucosal pathogens are being sought because 80–90% of infectious diseases are initiated at mucosal surfaces. However, our ability to deliver an intact vaccine antigen across a mucosal barrier for induction of effective immunity is limited. The neonatal Fc receptor (FcRn) mediates the transport of IgG across polarized epithelial cells lining mucosal surfaces. By mimicking IgG transfer at mucosal surfaces, intranasal immunization with a model antigen, herpes simplex virus type-2 (HSV-2) glycoprotein gD fused with an IgG Fc fragment, in combination with the adjuvant CpG, resulted in complete protection of wild type, but not FcRn knockout, mice that were intravaginally challenged with virulent HSV-2 186. This immunization strategy induced efficient mucosal and systemic antibody, B and T cell immune responses, including memory immune responses, which remained stable at least 6 months post-vaccination and conferred protection for a majority of animals. These results demonstrate that the FcRn-IgG transcellular transport pathway may represent a novel mucosal vaccine delivery route for a subunit vaccine against abundant mucosal pathogens.

Most pathogens initiate their infections through mucosal surfaces of the respiratory, gastrointestinal and urogenital tracts. An effective vaccine must therefore induce both mucosal and systemic immune responses to cope with early infection and pathogen spread 1–4. Delivery of vaccine antigens through the mucosal surface would be an ideal route to achieve mucosal, and potentially, systemic immunity because of the close association between mucosal epithelial cells and the immune effector cells within the lamina propria 1–3. However, epithelial monolayers lining the mucosal surfaces are impervious to macromolecule diffusion due to their intercellular tight junctions 5. In this way, the mucosal epithelium is a natural barrier for vaccine delivery. Different approaches have been explored to circumvent this problem, such as targeting mucosal vaccines onto differentiated microfold

Users may view, print, copy, download and text and data- mine the content in such documents, for the purposes of academic research, subject always to the full Conditions of use: http://www.nature.com/authors/editorial_policies/license.html#terms

²Address correspondence to: Dr. Xiaoping Zhu, VA-MD Regional College of Veterinary Medicine, University of Maryland, 8075 Greenmead Drive, College Park, MD 20742, USA. Phone: (301)314-6814; Fax: (301)314-6855; xzhu1@umd.edu.

Author Contributions L.Y. and X.Z. designed and performed experiments, analyzed data and wrote the paper. R.Z. and Y.B. conducted experiments. D.C.R. interpreted data and made editorial suggestions.

(M) cells that punctuate the mucosal epithelium 6. However, since columnar epithelial cells comprise the great majority of mucosal surfaces, alternative mucosal vaccine delivery strategies that target these abundant epithelial cells may increase the efficacy of mucosal vaccines.

The neonatal Fc receptor for IgG (FcRn), a MHC class I-related molecule, allows fetuses or newborns to obtain maternal IgG via the placental or intestinal route 7, 8. FcRn can also transport IgG antibody across mucosal surfaces in adult life 9–12 and lead to resistance to intestinal pathogens 12. Observations of IgG transport across mucosal epithelia by FcRn imply that FcRn may also transport an antigen, if fused with the IgG Fc, across the mucosal barrier. Therefore, FcRn-mediated mucosal vaccine delivery, if feasible, may allow the host to specifically sample an Fc-fused subunit vaccine in the mucosal lumen, followed by transport of an intact antigen across the mucosal epithelial barrier. To test this possibility, we used a model pathogen herpes simplex virus type-2 (HSV-2), which causes sexually-transmitted disease and initiates infection primarily at the mucosa of the genital tract 4. The development of HSV-2 subunit vaccine is mainly focused on its major envelope glycoprotein D (gD), because of its key role in the early steps of viral infection and its being major target for both humoral and cellular immunity. Therefore, in this study, we determined the ability of FcRn to deliver the model antigen, HSV-2 gD that plays key role in the early steps of viral infection and its being major target for both humoral and cellular immunity, across the mucosal barrier and further define protective immune responses and mechanisms relevant to this mode of mucosal vaccine delivery.

FcRn can efficiently transport intact subunit vaccine antigens across the respiratory mucosal barrier. To target gD to FcRn, we first generated the fusion protein, gD-Fc/wt, by cloning the extracellular domain of HSV-2 gD in frame with a modified form of the mouse IgG2a Fc fragment (Supplementary Fig. 1). We also generated a similarly modified gD-Fc/mut fusion protein that cannot not bind FcRn owing to H to A substitutions at positions 310 and 433 13. In both cases, the complement C1q-binding motif was eliminated to abrogate C1q binding 14 (Supplementary Fig. 1A). Comparison of these fusion proteins allowed us to evaluate the efficiency of FcRn-mediated transport and immunization efficacy. To ascertain whether the gD-Fc/wt but not the gD-Fc/mut fusion proteins were transported by FcRn, two criteria were applied. First, IMCD cells expressing FcRn 15 were evaluated for their ability to transport gD-Fc proteins in a transwell model. Indeed, FcRn-dependent transcytosis of intact gD-Fc/wt was detected in IMCD cells expressing FcRn 15 (Supplementary Fig. 2A). Second, we determined whether the gD-Fc/wt reached the bloodstream after intranasal (i.n.) inoculation. FcRn expression in mouse trachea and lung and its absence in the adult intestine were confirmed (Supplementary Fig. 2B). To investigate the ability of gD-Fc/wt, gD-Fc/mut and gD proteins to undergo mucosal transport in vivo, 20 µg of the these proteins were administered i.n. and their presence in serum was measured 8 hr later using an ELISA. In comparison with gD and gD-Fc/mut, gD-Fc/wt protein was abundantly detected in the sera of FcRn WT mice. Dependence on FcRn was further confirmed by the finding that the serum concentrations of gD-Fc/wt after administration into FcRn knockout (KO) mice 16 was greatly reduced as compared with that observed in FcRn WT mice (Supplementary Fig. 2C). These results showed that efficient delivery of gD across the respiratory barrier to the bloodstream was dependent on the Fc moiety and its ability to interact with FcRn.

Engagement of FcRn greatly increased the efficiency by which gD antigens induced antigen-specific antibody and cellular immune responses. We then determined whether FcRn-dependent transport augmented immune response potential of the gD protein. Mice were immunized i.n. with the gD-Fc, gD protein, or PBS, all in combination with CpG, and boosted after 2 wks. The gD unlinked to an Fc fragment allowed us to evaluate FcRn-independent effects *in vivo*, and also determine the magnitude of any observed enhancement in immune responses conferred by inclusion of the Fc and FcRn engagement. Given the tolerogenic potential of at least some immature dendritic cells (DCs) *in vivo*, we co-administrated CpG, a ligand for Toll-like receptor 9 (TLR-9), in an effort to overcome possible mucosal tolerance 17. In a different study, we found that co-administration of CpG ODN with an Fc fusion protein was required in order to induce a robust IgG response (unpublished data). We first measured antibody responses to gD in vaccinated animals at various time points up to 56 days. Significantly higher titers of IgG were seen in the gD-Fc/wt immunized mice when compared with the gD, gD-Fc/mut, gD-wt/KO immunized and PBS-treated groups (Fig. 1A). Moreover, sera from the gD-Fc/wt immunized mice exhibited strong neutralizing activity (Fig. 1B) and were able to most efficiently protect from intravaginal (ivag) challenge after passive transfer as compared with sera from all other groups (Supplementary Fig. 3). Likewise, gD-Fc/wt proteins induced strong IFN- γ -producing CD8⁺ and CD4⁺ T cell responses, as evidenced by significantly higher frequency of IFN- γ producing CD4⁺ (Fig. 1C) and CD8⁺ (Fig. 1C) T cells in response to gD stimulation in the spleens of FcRn WT mice immunized with gD-Fc/wt relative to the other groups. The cytokine responses were dominated by IFN- γ and IL-2 and with a lack of IL-4 production (Fig. 1D). This dominant Th1 cytokine response was also supported by a major IgG2a subclass in the sera of the immunized mice (Supplementary Fig. 4). It remains uncertain whether this polarized T cell response is caused by mucosal immunization as the result of FcRn targeting or, more likely, by the CpG used in as adjuvant, as CpG favorably induces Th1-type immune responses 17.

It is important to note that an important consequence of FcRn-targeted mucosal delivery of subunit vaccine was to elicit a strong mucosal immune response. This result is strongly supported by several lines of evidence. First, the nasopharynx-associated lymphoid tissue (NALT) and the mediastinal lymph nodes (MeLNs) draining the lung are usually the site where mucosal immune responses are initiated against antigens administered intranasally and reaching the lung 18. To ascertain the ability of the FcRn-targeted mucosal immunization to induce local humoral immune responses, we monitored the germinal center (GC) reaction in the MeLNs and spleens 10 days after the boost. Activated GCs are characterized by the presence of peanut agglutinin (PNA)-positive areas and high-level expression of Fas apoptotic death receptor in activated B cells 19. As shown in Fig. 2A, the gD-Fc/wt immunization induced a substantially higher of FAS⁺PNA⁺B220⁺ B cells in the MeLN or spleen in comparison with the percentages of other groups which was further validated by immunofluorescence imaging (Fig. 2B). In addition, the GC structure in the MeLNs in WT mice immunized by the gD-Fc/wt proteins was sustained much longer in comparison with that of other groups of the immunized animals (Fig. 2C). Administration of CpG alone failed to elicit appreciable GCs in the draining MeLNs, spleens, or lungs (Supplementary Fig. 5). The formation and maintenance of GC generally leads to the

differentiation of memory B cells and long-lived plasma cells. We also examined the mesenteric, cervical and inguinal lymph nodes and we failed to detect GC formation or the significant number of IFN γ secreting T cells at those sites. Second, it has been shown that i.n. administrated antigens can induce bronchus-associated lymphoid tissue (iBALT) in the lung, which is similar to GC structures 19. As shown in Fig. 2D, such GC-like structures could be detected in the lungs of gD-Fc/wt, but not gD-Fc/mut immunized mice or other groups of immunized animals (Supplementary Fig. 5) by co-localization of PNA- and B220-positive signals. It was also absent from other groups of immunized animals (Supplementary Fig. 5). Appearance of the GC in the iBALT in the lung is best explained by local induction due to the presence of the transported gD antigen in the MeLNs and lung, again emphasizing that the MeLNs play a major role as the inductive site. Third, antibodies, in particular IgA and IgG, represent the first defense line on mucosal surfaces. In order to assess the ability of FcRn-targeted mucosal immunization to induce gD-specific antibody in mucosal secretions, bronchial alveolar lavage (BAL) and vaginal washes were collected 10 days following the boost and analyzed for gD-specific IgG and IgA by ELISA. Significantly increased levels of gD-specific IgG were present in the BAL and vaginal washes (Supplementary Fig. 6) of the gD-Fc/wt protein immunized mice. WT, but not FcRn KO, mice that received the gD-Fc/wt had high levels of gD-specific IgG in BAL and vaginal washes ($p < 0.01$, Supplementary Fig. 6), suggesting the induction of mucosal IgG is FcRn-mediated. Of note is the observation that BAL- or vaginal IgG levels were much higher than that of IgA, despite high IgA levels in the nasal washings (Supplementary Fig. 6). Indeed, IgG appears a major isotype of immunoglobulin in the lower respiratory tract and reproductive tract. Fourth, with respect to T cell immune responses in the lung and MeLNs, 4 days after the boost we detected significantly higher frequency of IFN- γ producing CD4⁺ and CD8⁺ T cells (Figs. 2E and 2F) in response to gD stimulation in the mice immunized with the gD-Fc/wt in comparison with other groups. We conclude that antigen targeting to FcRn combined with the mucosal adjuvant CpG produced strong antibody as well as T cell mucosal immune responses. Considering that an efficient protective vaccine should induce immunity in the mucosa in order to hinder pathogen penetration and spreading, the data presented here suggest that FcRn-targeted mucosal immunization may provide an efficient approach for the development of protective mucosal vaccines.

Preferably, an effective mucosal subunit vaccine should also elicit both humoral and cell-mediated immunity not only at the mucosal delivery site, but also in systemic compartments that can access mucosal tissues distant from the immunization site 1–3. Studies have found that mucosal immunization using the intranasal route is effective for generating antibody and T cell immune responses in the female genital tract 1, 2, 4. Perhaps intranasal immunization stimulates cells in the NALT and its draining lymph nodes, leading to the migration of antibody secreting cells and T cells generated in the airway into the genital tract 20. We ivag challenged immunized mice with a lethal dose of HSV-2 186 strain 4 weeks following the boost. As expected, all PBS treated control mice succumbed to lethal infection. All FcRn wt mice immunized with the gD-Fc/wt survived with no obvious symptoms (Supplementary Fig. 7A), while gD-Fc/wt-immunized FcRn KO mice were incompletely protected (Fig. 3A). These data indicate that full protection is dependent on FcRn. Additionally, virus titers measured in the vaginal washes showed that the gD-Fc/wt

immunized mice had eliminated the virus by day 4 after challenge (Fig. 3B). In contrast, the other groups of mice essentially failed to control viral replication. Several immune mechanisms may account for the protection of the distal vaginal mucosa. First, both mucosal and systemic antibody responses may play an important protective role. This conclusion was supported by evidence that the sera passively transferred from the gD-Fc immunized mice conferred a high level of protection (Supplementary Fig. 3) and a significant amount of gD-specific IgG appeared in the vaginal secretions (Supplementary Fig. 6). IgG is a major protective antibody in mouse vaginal secretions after immunization with attenuated HSV-2 21. Second, T lymphocytes were present in the vaginal epithelium of HSV-2 challenged mice at a time coincident with virus clearance. IFN- γ is clearly indispensable for resistance to HSV-2 infections 20. The gD-Fc/wt protein induced a significantly higher frequency of IFN- γ producing CD4⁺ and CD8⁺ T cells in the vaginal tissues from the challenged mice (Fig. 3C) in comparison with other groups. The strong T cell response induced by FcRn targeted immunization could also provide resistance through direct lysis of MHC class I or II-bearing infected epithelial cells. Overall these results demonstrate that FcRn targeted mucosal immunization efficiently induced protective immunity.

FcRn targeted mucosal delivery of vaccine engendered an effective memory immune response. Immunological memory is characterized by increased levels of effector T and B cells and by the host's ability to respond faster and more vigorously to a second encounter with the pathogen or vaccine antigen 22 23. Hence, an important criterion for any vaccine is the formation and maintenance of a reservoir of memory lymphocytes with both adequate size and quality to maintain efficient immune surveillance for prolonged periods. Immunological memory 23 has been a concern in protein-based subunit mucosal vaccine development because preparations elicited levels of immunity immediately after vaccination but that immunity waned rapidly over time. However, a striking feature in this study is that FcRn targeted mucosal immunization promoted and sustained high levels of gD-specific plasma cells and memory B and T cells at least 6 months after the boost. This conclusion is strongly supported by several lines of evidence. First, gD-Fc/wt immunized mice developed significantly higher numbers of splenic memory B cells responsive to gD stimulation 6 months after the boost (Fig. 4A). By ELISPOT, we also found the significantly higher number of gD-specific IgG secreting plasma cells in the bone marrow of mice immunized with gD-Fc/wt in comparison with that of other groups (Fig. 4B and Supplementary Fig. 8). It remains to be determined if gD-specific IgA-secreting plasma cells also develop. Second, higher titers of gD-specific IgG were maintained for six months, the latest point tested after a boost in the mice immunized with the gD-Fc/wt, but high titers were not observed in groups that did not enable FcRn trafficking (Fig. 4C). Both the increase in GC and memory B cells in the spleen and the existence of long-lived plasma cells in the bone marrow niche can account for the maintenance of high levels of gD-specific IgG in circulation. Third, an important feature of memory T cells as opposed to the effector population is their proliferative potential upon reencounter with an antigen. We detected significant numbers of CD4⁺ (Fig. 4D, *upper panel*) and CD8⁺ (Fig. 4D, *bottom panel*) memory T cell proliferation by CFSE in response to gD recall in the mice immunized with gD-Fc/wt, but not in any of the other groups. This result was also verified by significantly increased numbers of actively proliferating T cells over time (Supplementary Fig. 9). These data indicate that the gD-

specific T cells had maintained a significant proliferative potential at least 6 months after the boost. Although the reason for the high memory T cell activity is not completely clear, IL-2-producing T cells formed in the responding T cell population (Supplementary Fig. 10) may be important since IL-2 plays an important role in the successful long-term survival of memory T cells *in vivo* 24. Fourth, to test if the memory immune response elicited from FcRn targeted mucosal immunization could provide protection, we again ivag challenged the immunized mice with a lethal dose of HSV-2 186 strain 6 months after the boost. Mice immunized with the gD-Fc/wt proteins exhibited less severe disease symptoms (Supplementary Fig. 7B) and had 80% survival (Fig. 4E), while the majority of mice in other groups succumbed to lethal mucosal infection.

Overall, this study shows that the FcRn/IgG transport pathway can be exploited to greatly enhance the efficacy of mucosally administered vaccines. Previous studies have taken advantage of Fc fusion proteins to augment the T cell immune response to myelin basic protein 25 and mucosally administered inactivated *Francisella tularensis*/antibody immune complexes have been shown enhance protection against the highly virulent strain of *F. tularensis* 26. We have shown that FcRn targeted mucosal immunization differs notably between WT and FcRn KO mice or the gD-Fc/wt and the gD-Fc/mut immunized mice in terms of mucosal and systemic immune responses, cytokine expression profiles, the maintenance of T and B cell memory and long lived bone marrow plasma cells, and resistance to infection. We establish this principle using a modified form of the mouse IgG2a Fc fragment to facilitate the vaccine antigen delivery across mucosal the barrier; whether FcRn dependent delivery of mucosal vaccines are as efficient using other subclasses of the IgG Fc fragment remain to be determined.

Earlier studies have shown intranasal and intravaginal immunization with gD or gB proteins in combination with CpG elicited immune responses and conferred partial protection to subsequent vaginal challenge with HSV-2 27–29. Lindqvist et al. 30 showed better protection, however, these mice were intranasally or intravaginally immunized three times by gD plus α -galactosylceramide. The mechanism by which “plain” gD or gB proteins crossed the airway or female genital epithelial barrier in those studies is not clear. Conditions that might explain passive mucosal transfer include the treatment of mice with agents that could compromise the integrity of the alveolo-capillary or mucosal epithelial barrier 31, 32, such use of volatile anesthetics or 0.5% Tween in α -galactosylceramide preparation 27–30. Moreover, injections with Depo-Provera before vaginal immunization 28–30 may affect tightness of the vaginal epithelial cells because Provera is a long-acting progesterone formulation and induces a diestrus-like state in genital tract of female mice 4. In agreement with a previous report 33, our other studies on examinations of the effect of CpG on protein transport across the nasal/tracheal mucosa (unpublished data) are not consistent with an affect of CpG on mucosal permeability or passive transfer. Regardless of the mechanism by which plain vaccine antigens may cross the mucosal barrier, our results clearly document the benefits of FcRn targeting to maximize the potential of mucosally administered vaccines to counteract mucosal pathogens, without the need for agents that may damage or otherwise compromise the integrity of mucosal barriers.

We suggest the following model for FcRn-targeted immunization (Fig. 4F). In general, mucosal DCs capture antigens in mucosal-associated lymphoid tissues, and subsequently migrate to draining lymph nodes where they can prime T cells 33, 34 and initiate the cognate B cell response. Persistence of vaccine antigens can facilitate long-term memory immune responses 22, 23. Thus, while FcRn-mediated transport is necessary for efficient vaccine proven necessary for effective mucosal immunization, the ability of FcRn to protect gD-Fc/wt proteins from degradation may further support the development of systemic immunity by increasing the persistence of gD-Fc/wt in circulation. Furthermore, this same protection property may augment long-term humoral immunity by maintaining serum high levels of IgG antibodies specific for gD-Fc/wt. It remains to be determined whether this delivery method can augment pre-existing immunity. Taken together, these results suggest that FcRn-targeted mucosal immunization could prove to be an effective strategy for maximizing the efficacy of vaccinations directed against a broad range of mucosal pathogens.

METHODS

Cells, antibodies, and virus

Inner Medullary Collecting Duct (IMCD) cell line and IMCD cells expressing rat FcRn were obtained from Dr. Neil Simister at Brandies University. Vero and Chinese hamster ovary (CHO-K) cells were purchased from American Tissue Culture Collection (ATCC). IMCD, Vero, and CHO cells were maintained in DMEM complete medium (Invitrogen Life Technologies) supplemented with 10 mM HEPES, 10% fetal bovine serum, 2 mM L-glutamine, nonessential amino acids, and penicillin (0.1 µg/ml)/streptomycin (0.292 µg/ml). Recombinant IMCD and CHO cells were grown under 400 µg/ml of G418 if necessary. Cells from spleen or bone marrow were grown in complete RPMI 1640 medium. Herpes Simplex Virus-2 (HSV-2) strain 186 was from Dr. Lawrence Stanberry (Columbia University, New York, NY) and HSV-2 stocks were prepared by infection of Vero cell monolayers at a multiplicity of infection (MOI) of 0.01. All cells and viruses were grown in a humidified atmosphere of 5% CO₂ at 37°C. Affinity purified antibody for mouse FcRn was made as previously described (30). HRP-conjugated donkey anti-rabbit or rabbit anti-mouse antibody was purchased from Pierce (Rockland). Purified mouse IgG and chicken IgY was from Rockland Laboratories, and HRP-conjugated goat anti-mouse IgG1, IgG2a and IgG3 were from Southern Biotech. All DNA modifying enzymes were purchased from New England Biolabs. Purified HSV-2 glycoprotein D was purchased from Meridian Life Science.

Expression of gD-Fc Fusion Proteins

The cDNA encoding the extracellular domain of HSV-2 gD (26–340 aa) was amplified by PCR from a plasmid provided by Dr. Patricia G. Spear (Northwestern University) using the primer pair (5'-cccaagcttaccatggggcggttgacctccggcgctc-3', 5'-agatcccagaccacctctccggaccacccccgcctgatccgccgggttgctggggg-3'). The antisense primer introduces an extension with fourteen codons for glycine and serine residues (GSGGGSGGGSGS). The Fc-fragment of mouse IgG2a containing the hinge, an extended CH2 and a CH3 domain was amplified by RT-PCR from the OKT3 hybridoma. The mouse IgG2a Fc fragment was used because mouse IgG2a, but not IgG1, is capable of binding mouse FcγRI, a high affinity

receptor for IgG. Similarly, the forward primer for IgG2a Fc has complementary glycine and serine codons for gD. A mutant Fc (HQ310 and HN433), unable to bind mouse FcRn, was made by oligonucleotide site-directed mutagenesis (Clontech) and designated as an Fc/mut. To construct a nonlytic Fc fragment, oligonucleotide site-directed mutagenesis was used to replace the C1q binding motif Glu318, Lys320, Lys322 with Ala residues 14. Fusions were then performed in a PCR-based gene assembly approach by mixing the cDNA for gD and the Fc fragment. All these DNA fragments were ligated into the pCDNA3 vector. Each construct was verified by DNA sequencing.

The plasmids containing the chimeric gD-Fc fragment were transfected into CHO cells. G418-resistant clones were selected for secretion of gD-Fc fusion protein. SDS-PAGE and Western blot were performed to assess the recombinant fusion proteins in serum-free medium (Invitrogen). The highest secreting clones were screened. Recombinant proteins were purified from CHO cell supernatants by affinity chromatography using Protein A Sepharose 4 Fast Flow (Amersham) or goat anti-mouse IgG affinity column (Rockland). Protein concentration was measured with Coomassie (Bradford) protein assay kit (Pierce) using mouse IgG2a as standard.

Western blot and SDS-PAGE gel electrophoresis

The proteins or cell lysates were resolved on a 12% SDS-PAGE gel under a reducing or non-reducing condition. Proteins were transferred onto a nitrocellulose membrane (Schleicher & Schuell). The membranes were blocked with 5% non-fat milk, probed separately with anti-gD, anti-IgG Fc Ab or anti-mouse FcRn for 1 hr, and followed by incubation with HRP-conjugated rabbit anti-mouse or donkey anti-rabbit Ab. All blocking, incubation, and washing were performed in PBST solution (PBS and 0.05% Tween 20). Proteins were visualized by ECL (Pierce).

In vitro and in vivo transcytosis

The *in vitro* IgG transport assay was performed as a modification from previously-described methods 15, 36. IMCD cells expressing rat FcRn were grown on transwell filter inserts (Corning Costar) to form a monolayer exhibiting transepithelial electrical resistances (TER, $300 \Omega \cdot \text{cm}^2$). TER was measured using a tissue-resistance measurement equipped with planar electrodes (World Precision Instruments). Monolayers were equilibrated in Hanks' balanced salt solution. Fusion proteins (50 $\mu\text{g}/\text{ml}$) were applied to the apical compartment, and incubated with DMEM medium supplied with or without 1mg/ml of mouse IgG or chicken IgY as competitors for 2 hr at 37°C degree. Transported proteins were sampled from the basolateral chamber and analyzed by reducing SDS-PAGE and Western blot-ECL. For *in vivo* transport, the biotinylated 20 μg of fusion proteins or gD alone in 20 μl of PBS were administered intranasally (i.n.) into the mice that were anesthetized with 100 μl of avertin (40mg/ml). 8 hr later or at indicated time points, transported proteins in sera were determined by ELISA.

Mouse immunization and virus challenge

Six to eight week-old Female inbred C57BL/6 mice were purchased from Charles River. FcRn knockout mice on a C57BL/6 background 16 were from the Jackson Laboratory. All

mice were housed in the animal resources facility at the University of Maryland. All animal studies were reviewed and approved by the Institutional Animal Care and Use Committee. To overcome the possible mucosal immune tolerance 37, all proteins and PBS were mixed with immunostimulatory DNA rich in CG motifs CpG ODN 1826 (abbreviated CpG). Groups of 5 mice were intranasally immunized with 20 μ l of 20 μ g gD-Fc/wt, gD-Fc/mut, or recombinant gD alone in combination with 20 μ g CpG (5'-TCCATGACGTTCCCTGACGTT-3') (Invivogen) per immunization at weeks 0 and 2 with an intraperitoneal injection of 100 μ l of avertin (40 mg/ml). An additional group of 5 mice was mock-immunized with PBS following the same schedule. Mice were kept on their backs under anesthesia to allow the inoculum to be taken up.

Mice were inoculated with viruses intravaginally as described previously 27, 38. Briefly, prior to inoculation, each mouse was subcutaneously treated with 3 mg of medroxyprogesterone acetate (Depo-Provera) 10 days prior to virus inoculation. Hormonal pretreatment was necessary to induce susceptibility of mice to genital HSV-2 inoculation, which may reflect thinning of the genital epithelium or induction of the HSV entry receptor, nectin-1, on vaginal epithelial cells. Mice anesthetized by avertin (40 mg/ml, Sigma) were infected intravaginally with 1×10^4 pfu/100 μ l of HSV-2 strain 186. Mice were kept on their backs under the influence of anesthesia for 45 min to allow infection. Mice were monitored for 15 days for the disease and death. Mice exhibiting severe disease symptom were euthanized. For virus titration, virus was inoculated into Vero cells and incubated for 45 min at 37°C. The cells were washed and DMEM containing 0.8% methcellulose and 2% FBS was added to overlay the cells. The cells were cultured for 3 days, the overlay was removed, and the cells were fixed with 3.7% formaldehyde for 1 hr, and stained with 1% crystal violet.

Preparation of single-cell suspensions from lymph nodes, spleen, lung, and vaginal tissues

Spleens and lymph nodes 39 were made into single-cell suspensions by passage through a sterile mesh screen. Cells were resuspended in Hanks' balanced salt solution (HBSS) and counted by trypan blue dye exclusion. For each experiment, cells were generally pooled from 3–5 mice in each group. For preparation of single-cell suspension from the lung, mice were anesthetized with 400 μ l of avertin (40mg/ml) by i.p. injection. Lungs were perfused with 10 ml PBS through the right ventricle, removed, minced with blades, and incubated with HBSS containing 2.5 mM HEPES and 1.3 mM EDTA at 37°C for 30 min, followed by treatment at 37°C for 1 hr with 2.5 mg/ml collengase D (Roche) in RPMI 1640 medium containing 5% FBS. The resulting cells were filtered through a 70- μ m cell strainer (BD) and used for FACS analysis.

For isolation of vaginal cells, the vagina was excised, cut longitudinally, and minced with a sterile scalpel in complete RPMI 1640 culture medium. Minced tissues (epithelium and lamina propria) were digested in complete medium with sterile 0.25% collagenase D (Sigma). Digestion was accomplished with shaking incubation at 37°C for 30 min. After digestion, tissues and cells were filtered through a sterile gauze mesh and washed with RPMI 1640 medium, and additional tissue debris was excluded by slow-speed centrifugation

for 1 min. Cells were collected from the supernatant by centrifugation, resuspended in HBSS, and counted by trypan blue dye exclusion.

Flow cytometry

Single cell suspensions from the spleen, lung or vaginal tissues were collected and cells were spun down. Erythrocytes were then lysed in 0.14 M NH_4Cl , 0.017 M Tris-HCl at pH 7.2 on ice for 5 min. Cells were preincubated with an Fc block (mAb to CD16–CD32, 2.4G2, PharMingen) and washed in FACS buffer (HBSS, 2% bovine serum albumin, 0.01% sodium azide). Cells were incubated with specific antibody (0.25 $\mu\text{g}/10^6$ cells/100 μl) directly conjugated to fluorescein isothiocyanate (FITC), phycoerythrin (PE), washed, transferred to FACS buffer, and analyzed using a FACSAire (Becton Dickinson, Mountain View, CA) and FlowJo software (Tree Star). The mAbs (PharMingen) we used were anti-CD3 ϵ , 500A2; anti-CD4, RM4-5; anti-CD8, 53-6.7; anti-IFN- γ , XMG1.2; anti-B220, RA3-6B2; FAS, Jo2; CD19, 1D3. PNA was from Sigma. Purified HSV-2 gD proteins were labeled with Alexa Fluoro647 protein labeling kit (Invitrogen) according to the manufacturer's instruction. Cells incubated with isotype control antibodies were used to determine the background fluorescence. The isotype control antibodies included in each experiment were considered the true baseline fluorescence used to evaluate and illustrate the results for the cell-specific antigen markers.

T cell proliferation

Single cell suspensions from mouse spleen were suspended in RPMI-1640 with 1% FCS, 2.5mM Hepes at $10^7/\text{ml}$. Carboxyfluorescein diacetate succinimidyl ester (CFSE, 5mM stock, Invitrogen) was 10-fold diluted with PBS, 4 μl of diluted CFSE was then added into $10^7/\text{ml}$ cells for a 2 μM final concentration. The reaction was incubated for 10 min at 37°C. Cold FBS (1 ml) was added and incubated on ice for 5 min to stop the reaction. The cells were washed twice with RPMI-1640 with 10% FCS. Labeled cells (5×10^5) were plated into 96 well plates in 200 μl of medium and cultured for 5 days. The cells were then harvested and subjected to flow cytometry assay.

Intracellular cytokine staining

Intracellular IFN- γ production by primed CD4 $^+$ and CD8 $^+$ T cells was evaluated using bulk splenocytes or isolated lung or vaginal infiltrating lymphocytes incubated for 4 hr with 25 $\mu\text{g}/\text{ml}$ of the purified gD protein or medium alone. Cells were then cultured for another 6 hr in the presence of brefeldin A (Sigma). The cells were then washed and incubated with anti-CD16/CD32 antibody to block Fc γ receptors, and stained with anti-mouse CD4, CD8, and CD3 antibodies for 15 min at 4°C. After fixation and membrane penetration with Cytofix/Cytoperm Plus (BD Biosciences), cells were stained for intracellular IFN- γ for 30 min on ice. Cells were washed three times, resuspended in FACS buffer, and analyzed by flow cytometry.

Enzyme-linked immunosorbent assay (ELISA), enzyme-linked immunosorbent spot (ELISPOT), and neutralization test

For the detection of gD-specific antibodies in serum, bronchial lavage and vaginal fluid, high-binding ELISA plates (Maxisorp, Nunc) were coated with 5 µg/ml of recombinant gD protein in PBS and incubated overnight at 4°C. Plates were then washed three times with 0.02% Tween 20 in PBS and blocked with 1% BSA in PBS for 1 hr at room temperature. Samples were serially diluted in 0.25% BSA-PBS and incubated for 2 hr at room temperature. HRP-conjugated rabbit anti-mouse IgG antibody (1:2,000, Pierce) or anti-mouse subclass-specific antibodies (1:5000, SouthernBiotech) was added and followed by colorimetric assay using substrate tetramethyl benzidine and a Victor III microplate reader (Perkin Elmer). Titers represent the highest dilution of samples showing a 2-fold OD₄₅₀ value over controls. Neutralizing antibodies were measured by a standard virus neutralization assay. Sera were heat-inactivated, diluted 10-fold, then in two-fold steps in MEM with 2% FBS. Fifty PFU of HSV-2 was added per well and incubated at 37°C for 1 hr. Then, plaque assays were performed. The titers were expressed as the reciprocal of the twofold serial dilution preventing the appearance of the CPE. Each assay was done in triplicate.

For measuring gD-specific antibody-producing plasma cells, the 96-well ELISPOT plates (Millipore) were coated with 5 µg/ml gD and blocked with RPMI 5% FCS (Invitrogen) for 90 min at 37°C and 5% CO₂. Serial dilutions of bone marrow single-cell suspensions were prepared in RPMI and incubated in the coated wells for 24 hr at 37°C in 5% CO₂. Cells were removed, and plates were washed 5 times with 0.1% Tween 20 in PBS, then incubated with biotin labeled goat anti-mouse IgG-specific antibody (1:1500, Sigma) for 2 hr. After washing the cells, with PBS, the avidin conjugated HRP (1:2,000, Vector Laboratories) was added and incubated for 1 hr, followed by substrate from the AEC kit (BD Biosciences). Spots were counted with ELISPOT Reader and analyzed with software (Zesis). Mouse cytokines IFN-γ, IL-2, and IL-4 from the cell culture supernatant were analyzed by ELISA according to the manufacturer's instructions (BD Biosciences).

Immunofluorescence

Immunofluorescence was performed as previously described 40. Briefly, frozen serial sections of tissues were cold-fixed in acetone for 3 min at 4°C and blocked with 10% normal goat serum and stained with biotin-PNA (germinal centers, red), Alexa 647-IgD or anti-B220 (B cells, green), followed by Alexa 555-avidin or 488 Fluoro-conjugated IgG of the corresponding species. After each step, cells were washed at least three times with 0.1% Tween-20 in PBS. Cover slips were mounted on slides with Prolong TM intifada kit (Molecular Probes) and examined using a Zees LSM 510 confocal fluorescence microscopy. Images were processed by Adobe Photoshop 7.0.

Passive transfer of immune sera

Sera were collected from 3–5 mice per group 4 weeks after the immunization, then pooled, heat inactivated and stored frozen at –80°C until use. Mice received a single intraperitoneal (i.p.) injection of 0.3 ml immune sera 3 days prior to challenge to allow distribution and

equilibration of antibody to all tissues prior to virus inoculation. Mice were challenged intravaginally with 1×10^4 PFU HSV-2 186 strain.

Statistics analysis

To compare survival curves, Kaplan-Meier log-rank analyses were used. Antibody titers, serum gD concentration, cytokine concentration and virus titers were assessed by using the unpaired two-tailed t test. Graph Pad Prism 5 provided the software for the statistical analysis.

Supplementary Material

Refer to Web version on PubMed Central for supplementary material.

Acknowledgements

We thank Dr. Kenneth Rosenthal and Dr. Ali Harandi for their discussions of mucosal antigen transport and immunization. We thank Dr. Geoffrey J. Letchworth for helpful discussions and critical reading of the manuscript. We are grateful to Dr. Neil E. Simister for supplying us with IMCD-FcRn cell line. We acknowledge the receipt of HSV-2 186 strain from Dr. Lawrence R. Stanberry and HSV gD plasmids from Dr. Patricia Spear. We also acknowledge the helpful discussions with Dr. David Mosser, Dr. Daniel Perez, Dr. Siba Samal, and Dr. Wenxia Song. We are most grateful for the technical help from Dr. Yunsheng Wang, Dr. Li Lu, Dr. Xindong Liu, Senthilkumar Palaniyandi, and Dr. Zili Li.

This work was supported, in part by the National Institutes of Health grants AI65892, AI67965, AI73139 (to X. Z.), DK56597 (to D.C.R.), and MAES competitive grants from the University of Maryland (to X. Z.).

The abbreviations used in this paper

CFSE	carboxyfluorescein diacetate succinimidyl ester
HSV	herpes simplex virus
IMCD	inner medullary collecting duct
MHC	major histocompatibility complex
FcRn	neonatal Fc receptor
β_2m	β_2 -microglobulin

References

1. Neutra MR, Kozlowski PA. Mucosal vaccines: the promise and the challenge. *Nat. Rev. Immunol.* 2006; 6:148–158. [PubMed: 16491139]
2. Holmgren J, Czerkinsky C. Mucosal immunity and vaccines. *Nat. Med.* 2005; 11(4 Suppl):S45–S53. [PubMed: 15812489]
3. McGhee JR, et al. The mucosal immune system: from fundamental concepts to vaccine development. *Vaccine.* 1992; 10:75–88. [PubMed: 1539467]
4. Gallichan WS, Rosenthal KL. Long-term immunity and protection against herpes simplex virus type 2 in the murine female genital tract after mucosal but not systemic immunization. *J. Infect. Dis.* 1988; 177:1155–1161. [PubMed: 9592997]
5. Neutra MR, Mantis NJ, Kraehenbuhl J-P. Collaboration of epithelial cells with organized mucosal lymphoid tissues. *Nat. Immunol.* 2001; 2:1004–1009. [PubMed: 11685223]

6. Nochi T, et al. A novel M cell-specific carbohydrate-targeted mucosal vaccine effectively induces antigen-specific immune responses. *J. Exp. Med.* 2007; 204:2789–2796. [PubMed: 17984304]
7. Ghetie V, Ward ES. Multiple roles for the major histocompatibility complex class I-related receptor FcRn. *Annu. Rev. Immunol.* 2000; 18:739–766. [PubMed: 10837074]
8. He W, et al. FcRn-mediated antibody transport across epithelial cells revealed by electron tomography. *Nature.* 2008; 455:542–546. [PubMed: 18818657]
9. Dickinson BL, et al. Bidirectional FcRn-dependent IgG transport in a polarized human intestinal epithelial cell line. *J. Clin. Invest.* 1999; 104:903–911. [PubMed: 10510331]
10. Roopenian DC, Akilesh S. FcRn: the neonatal Fc receptor comes of age. *Nat. Rev. Immunol.* 2007; 7:715–725. [PubMed: 17703228]
11. Baker K, et al. Immune and non-immune functions of the (not so) neonatal Fc receptor, FcRn. *Semin. Immunopathol.* 2009:223–236. [PubMed: 19495758]
12. Yoshida M, et al. Neonatal Fc receptor for IgG regulates mucosal immune responses to luminal bacteria. *J. Clin. Invest.* 2006; 116:2142–2151. [PubMed: 16841095]
13. Kim JK, Tsen MF, Ghetie V, Ward ES. Localization of the site of the murine IgG1 molecule that is involved in binding to the murine intestinal Fc receptor. *Eur. J. Immunol.* 1994; 24:2429–2434. [PubMed: 7925571]
14. Duncan AR, Winter G. The binding site for C1q on IgG. *Nature.* 1988; 332:738–740. [PubMed: 3258649]
15. McCarthy KM, Yoong Y, Simister NE. Bidirectional transcytosis of IgG by the rat neonatal Fc receptor expressed in a rat kidney cell line: a system to study protein transport across epithelia. *J. Cell Sci.* 2000; 113:1277–1285. [PubMed: 10704378]
16. Roopenian DC, et al. The MHC class I-like IgG receptor controls perinatal IgG transport, IgG homeostasis, and fate of IgG-Fc-coupled drugs. *J. Immunol.* 2003; 170:3528–3533. [PubMed: 12646614]
17. van Duin D, Medzhitov R, Shaw AC. Triggering TLR signaling in vaccination. *Trends Immunol.* 2006; 27:49–55. [PubMed: 16310411]
18. Wolf AJ, et al. Initiation of the adaptive immune response to *Mycobacterium tuberculosis* depends on antigen production in the local lymph node, not the lungs. *J. Exp. Med.* 2008; 205:105–115. [PubMed: 18158321]
19. Moyron-Quiroz JE, et al. Role of inducible bronchus associated lymphoid tissue (iBALT) in respiratory immunity. *Nat. Med.* 2004; 10:927–934. [PubMed: 15311275]
20. Milligan GN, Dudley-McClain KL, Chu CF, Young CG. Efficacy of genital T cell responses to herpes simplex virus type 2 resulting from immunization of the nasal mucosa. *Virology.* 2004; 318:507–515. [PubMed: 14972519]
21. Parr EL, Parr MB. Immunoglobulin G is the main protective antibody in mouse vaginal secretions after vaginal immunization with attenuated herpes simplex virus type 2. *J. Virol.* 1997; 71:8109–9115. [PubMed: 9343160]
22. Ahmed R, Gray D. Immunological memory and protective immunity: understanding their relation. *Science.* 1996; 272:54–60. [PubMed: 8600537]
23. Bernasconi NL, Traggiai E, Lanzavecchia A. Maintenance of serological memory by polyclonal activation of human memory B cells. *Science.* 2002; 298:2199–2202. [PubMed: 12481138]
24. Doms H, Wolslegel K, Lin P, Abbas AK. Interleukin-2 enhances CD4⁺ T cell memory by promoting the generation of IL-7R α -expressing cells. *J. Exp. Med.* 2007; 204:547–557. [PubMed: 17312008]
25. Mi W, et al. Targeting the neonatal Fc receptor for antigen delivery using engineered Fc fragments. *J Immunol.* 2008; 181:7550–7561. [PubMed: 19017944]
26. Rawool DB, et al. Utilization of Fc receptors as a mucosal vaccine strategy against an intracellular bacterium, *Francisella tularensis*. *J. Immunol.* 2008; 180:5548–5557. [PubMed: 18390739]
27. Gallichan WS, et al. Intranasal immunization with CpG oligodeoxynucleotides as an adjuvant dramatically increases IgA and protection against herpes simplex virus-2 in the genital tract. *J. Immunol.* 2001; 166:3451–3457. [PubMed: 11207303]

28. Kwant A, Rosenthal KL. Intravaginal immunization with viral subunit protein plus CpG oligodeoxynucleotides induces protective immunity against HSV-2. *Vaccine*. 2004; 22:3098–3104. [PubMed: 15297061]
29. Tengvall S, Lundqvist A, Eisenberg RJ, Cohen GH, Harandi AM. Mucosal administration of CpG oligodeoxynucleotide elicits strong CC and CXC chemokine responses in the vagina and serves as a potent Th1-tilting adjuvant for recombinant gD2 protein vaccination against genital herpes. *J. Virol*. 2006; 80:5283–5291. [PubMed: 16699008]
30. Lindqvist M, Persson J, Thörn K, Harandi AM. The mucosal adjuvant effect of alpha-galactosylceramide for induction of protective immunity to sexually transmitted viral infection. *J. Immunol*. 2009; 182:6435–6443. [PubMed: 19414797]
31. ChangLai SP, Hung WT, Liao KK. Detecting alveolar epithelial injury following volatile anesthetics by (99m)Tc DTPA radioaerosol inhalation lung scan. *Respiration*. 1999; 66:506–510. [PubMed: 10575335]
32. Lin H, et al. Enhancing effect of surfactants on fexofenadine.HCl transport across the human nasal epithelial cell monolayer. *Int. J. Pharm*. 2007; 330:23–31. [PubMed: 16997520]
33. Kodama S, Abe N, Hirano T, Suzuki M. Safety and efficacy of nasal application of CpG oligodeoxynucleotide as a mucosal adjuvant. *Laryngoscope*. 2006; 116:331–335. [PubMed: 16467729]
34. Kelsall BL, Rescigno M. Mucosal dendritic cells in immunity and inflammation. *Nat. Immunol*. 2004; 5:1091–1095. [PubMed: 15496943]
35. Yoshida M, et al. Human neonatal Fc receptor mediates transport of IgG into luminal secretions for delivery of antigens to mucosal dendritic cells. *Immunity*. 2004; 20:76–783.
36. Liu X, et al. Activation of the JAK/STAT-1 signaling pathway by IFN-gamma can down-regulate functional expression of the MHC class I-related neonatal Fc receptor for IgG. *J. Immunol*. 2008; 181:449–463. [PubMed: 18566411]
37. Mestecky J, Russell JNW, Elson CO. Perspectives on mucosal vaccines: is mucosal tolerance a barrier? *J. Immunol*. 2007; 179:5633–5638. [PubMed: 17947632]
38. Milligan GN, Bernstein DI, Bourne NT. lymphocytes are required for protection of the vaginal mucosae and sensory ganglia of immune mice against reinfection with herpes simplex virus type 2. *J. Immunol*. 1998; 160:6093–6100. [PubMed: 9637526]
39. Van den Broeck W, Derore A, Simoens P. Anatomy and nomenclature of murine lymph nodes: Descriptive study and nomenclatory standardization in BALB/cAnNCrl mice. *J. Immunol. Methods*. 2006; 312:12–19. [PubMed: 16624319]
40. Ye L, et al. The MHC class II-associated invariant chain interacts with the neonatal Fc gamma receptor and modulates its trafficking to endosomal/lysosomal compartments. *J. Immunol*. 2008; 181:2572–2585. [PubMed: 18684948]

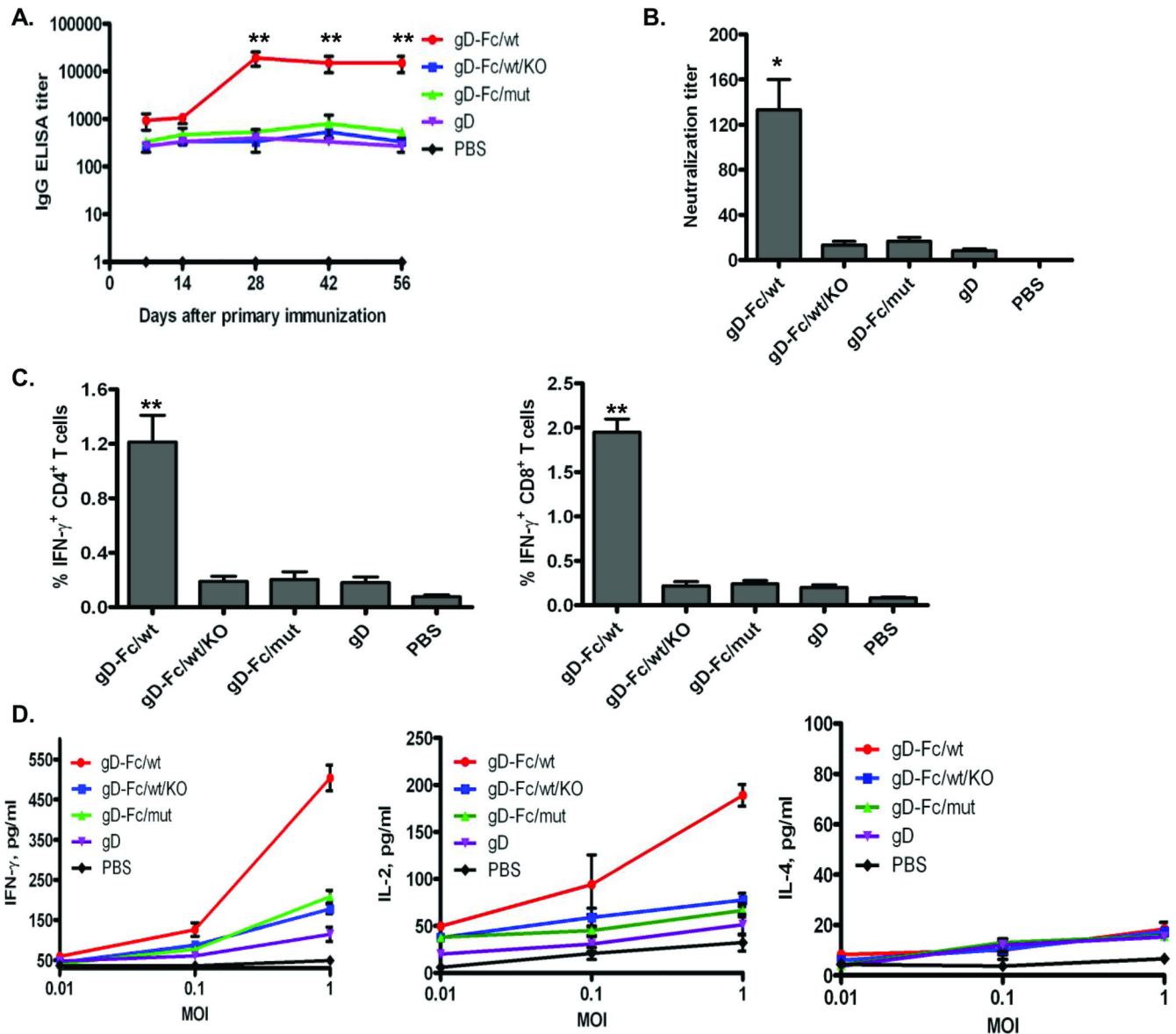


Fig. 1. FcRn-targeted mucosal vaccination induces enhanced gD-specific antibody and T cell responses

The 20 μ g gD-Fc/wt, gD-Fc/mut, gD, or PBS in combination with 20 μ g CpG were i.n. administered into wild-type (WT) or FcRn knockout (KO) mice.

(A). Measurement of anti-HSV-2 gD-specific IgG antibody titers in serum before and after the boost immunization. HSV-2 gD-specific IgG antibody at indicated days was measured in serum by ELISA. Immunization conditions are displayed at the right. The curves represent mean values for each group (\pm S.E.M.). Values marked with asterisk in this and subsequent figures: * P < 0.05; ** P < 0.01.

(B). Test of neutralizing activity in the immunized sera. Sera were heat-inactivated, diluted 10-fold, then in twofold steps in MEM with 2% FBS. HSV-2 (50 PFU) was added and incubated at 37°C for 1 hr. Finally, the mixture were removed and washed, overlaid with 0.8% methylcellulose in 2% FBS containing DMEM and further incubated for 72 hr at

37°C. The titers were expressed as the reciprocal of the twofold serial dilution preventing the appearance of the cytopathic effects (CPE) over control sera. Each assay was done in triplicate.

(C). The percentage of IFN- γ producing T cells in the spleen 4 days after the boost. Spleen cells from the immunized mice were stimulated for 10 hr with purified gD or medium control. Lymphocytes were gated by forward and side scatter and T cells labeled with anti-CD3 and identified by their respective surface markers CD4 and CD8 and intracellular IFN- γ staining. Immunization conditions are displayed on the bottom. Numbers represent the percentage of IFN- γ^+ CD3 $^+$ CD4 $^+$ (left panel) or IFN- γ^+ CD3 $^+$ CD8 $^+$ (right panel) T cells. Isotype controls included FITC-mouse-IgG1 with baseline response.

(D) Cytokine secretions from the stimulated spleen T cells. Spleen cells were collected on day 4 after the boost. Cells were stimulated *in vitro* specifically with different multiplicity of infection (MOI) of inactivated HSV-2 virus as indicated for 24 hr. Cytokines IFN- γ , IL-2, and IL-4 in the culture supernatant were detected by ELISA. Data are representative of three experiments with three immunized mice pooled in each group.

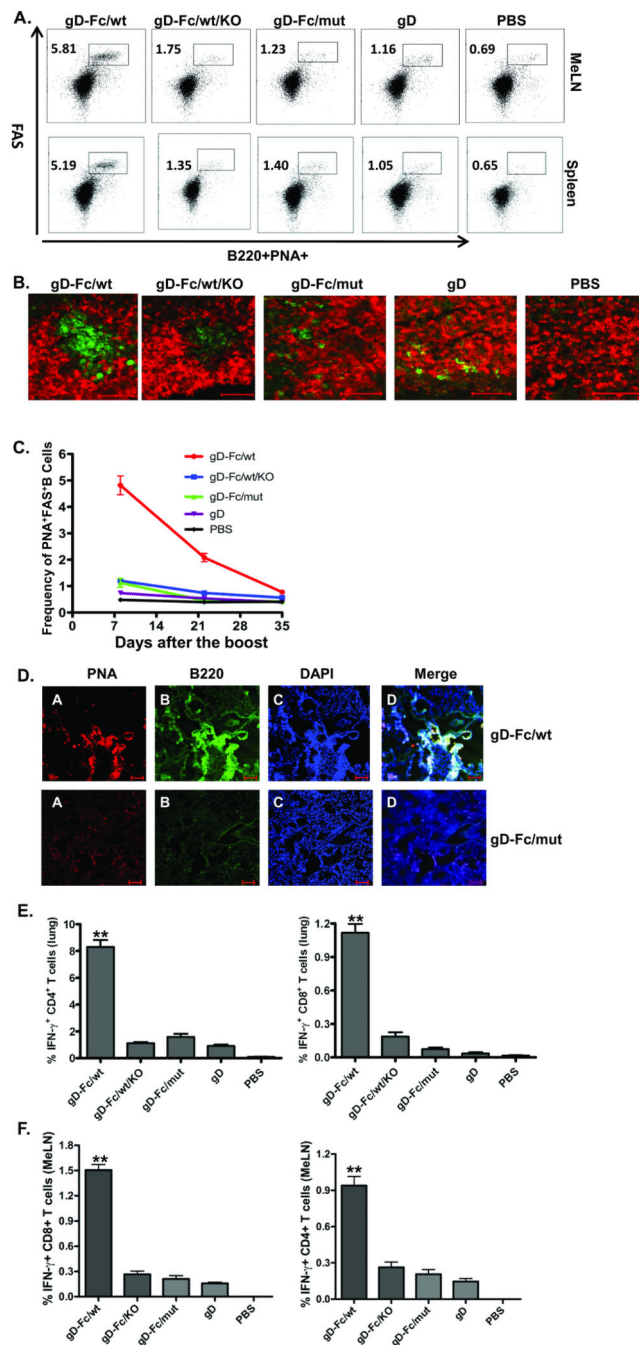


Fig. 2. Local immune responses induced by FcRn-targeted mucosal immunization

(A). Accumulation of activated B cells in germinal centers (GCs) in the mediastinal lymph nodes (MeLNs) and spleen. Representative flow cytometric analyses of GC B cells among CD19⁺B220⁺ B cells in the MeLNs and spleen 10 days after the boost. B220⁺PNA^{high} cells are B cells that exhibit the phenotypic attributes of GC B cells. The GC staining in spleen was used as a positive control. Numbers are the percentage of activated GC B cells (PNA⁺FAS⁺) among gated B cells and are representative of three independent experiments.

(B). GC formation and presence of activated B cells following immunizations as indicated. Frozen MeLN sections at day 10 from the immunized mice were co-stained with biotin–PNA (developed with avidin–FITC) and Alexa647 labeled anti-IgD. Scale bar represents 50 μm .

(C). Quantitative analysis of GCs following immunization. The dynamics of the frequency of germinal center B cells (FAS+PNA+, gated on CD19+B220+ cells) were plotted on day 10, 22 and 35 after the boost. Data indicate the mean and S.E.M., n=5 mice.

(D). The formation of inducible bronchus-associated lymphoid tissue (iBALT). Frozen serial sections of the lung were stained with biotin-PNA (GC, red) and anti-B220 (B cells, green), followed by Alexa 488-conjugated IgG of corresponding species and Alexa 555-Avidin. The nucleus is stained with DAPI (blue). A germinal center-like structure is shown in the merged panel by the white color. The data are representative of sections from at least three independent mice. Images were originally obtained at 10 \times magnification. Scale bars represent 100 μm .

(E) + (F). Presence of HSV-2 gD-specific T lymphocytes in the lung (E) and MeLNs (F). Lung or MeLN cells from mice 4 days after the boost were collected. Lymphocytes were gated based on their forward scatter (FSC) vs. side scatter (SSC) profile. Intracellular staining for IFN- γ was performed after surface staining of CD4 and CD8 molecules. The profiles shown are representative of five mice from three separate experiments. Numbers indicate percentages of IFN- γ -producing T lymphocytes from gated CD4⁺ and CD8⁺ T cells.

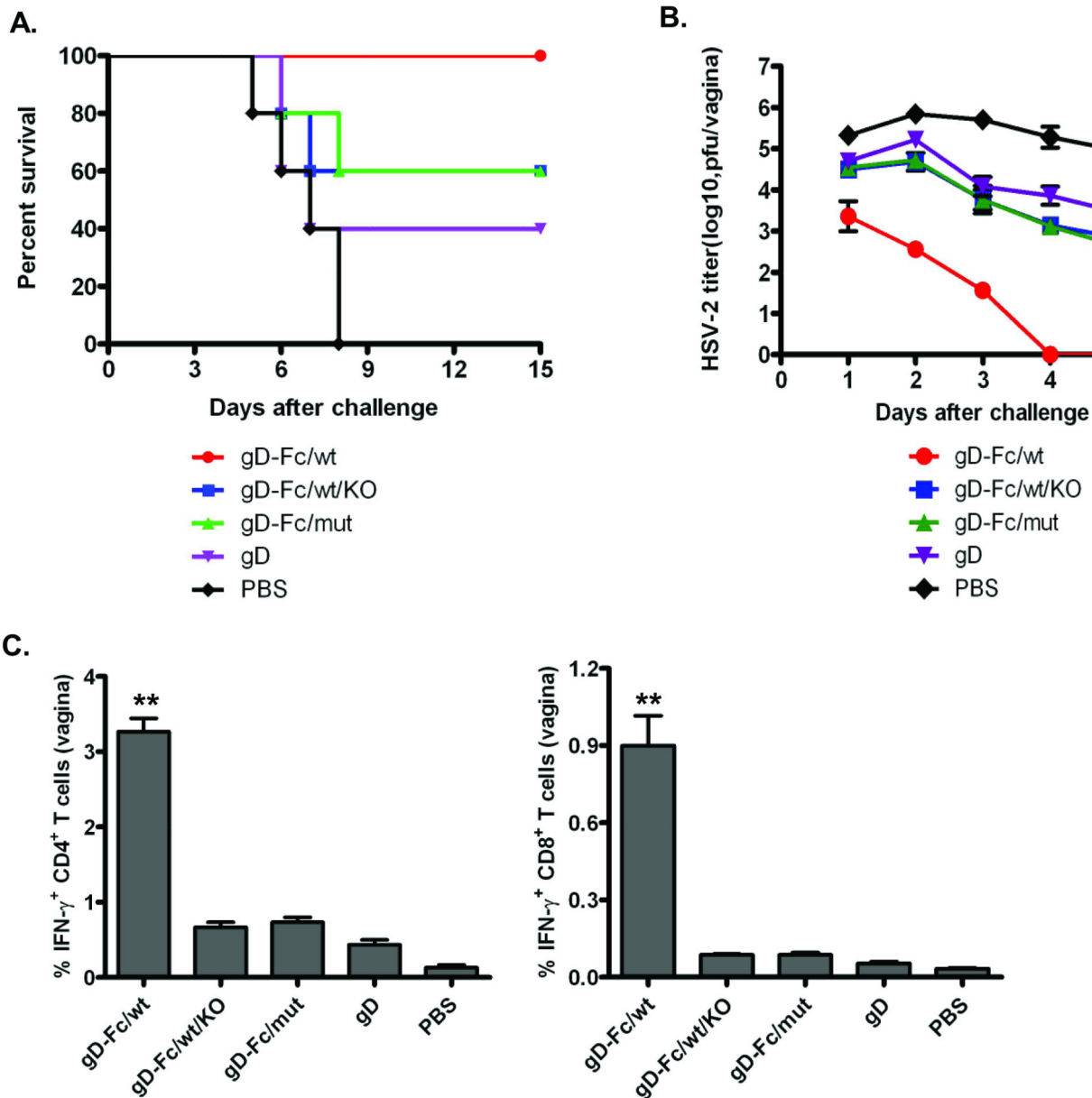


Fig. 3. FcRn-targeted mucosal immunization provides protective immunity to intravaginal (ivag) challenge with virulent HSV-2 186

(A) Mean survival following genital HSV-2 challenge. Four weeks after the immunization, groups of five mice were challenged intravaginally with 1×10^4 pfu of HSV-2 strain 186. Percentage of mice from protection on the indicated days is calculated as the number of mice surviving divided by the number of mice in each group and represented two similar experiments.

(B) Mean of viral titers following HSV-2 challenge. Virus titers were measured from vaginal washes by taking swabs on the indicated days after HSV-2 inoculation based on a plaque assay on Vero cell monolayers.

(C). Increased presence of HSV-specific T lymphocytes in the vaginal epithelium after challenge. Lymphocytes were harvested from collagenase-digested vaginal tissues 4 days

intravaginal inoculation of virus. Intracellular staining for IFN- γ expression on CD4⁺ and CD8⁺ T cells was analyzed after gating on viable CD3⁺ lymphocytes. The numbers in each column show the percentage of IFN- γ -positive T lymphocytes from the gated CD4⁺ or CD8⁺ T cells. Data shown are of a representative from three experiments using 3 mice per experiment.

Author Manuscript

Author Manuscript

Author Manuscript

Author Manuscript

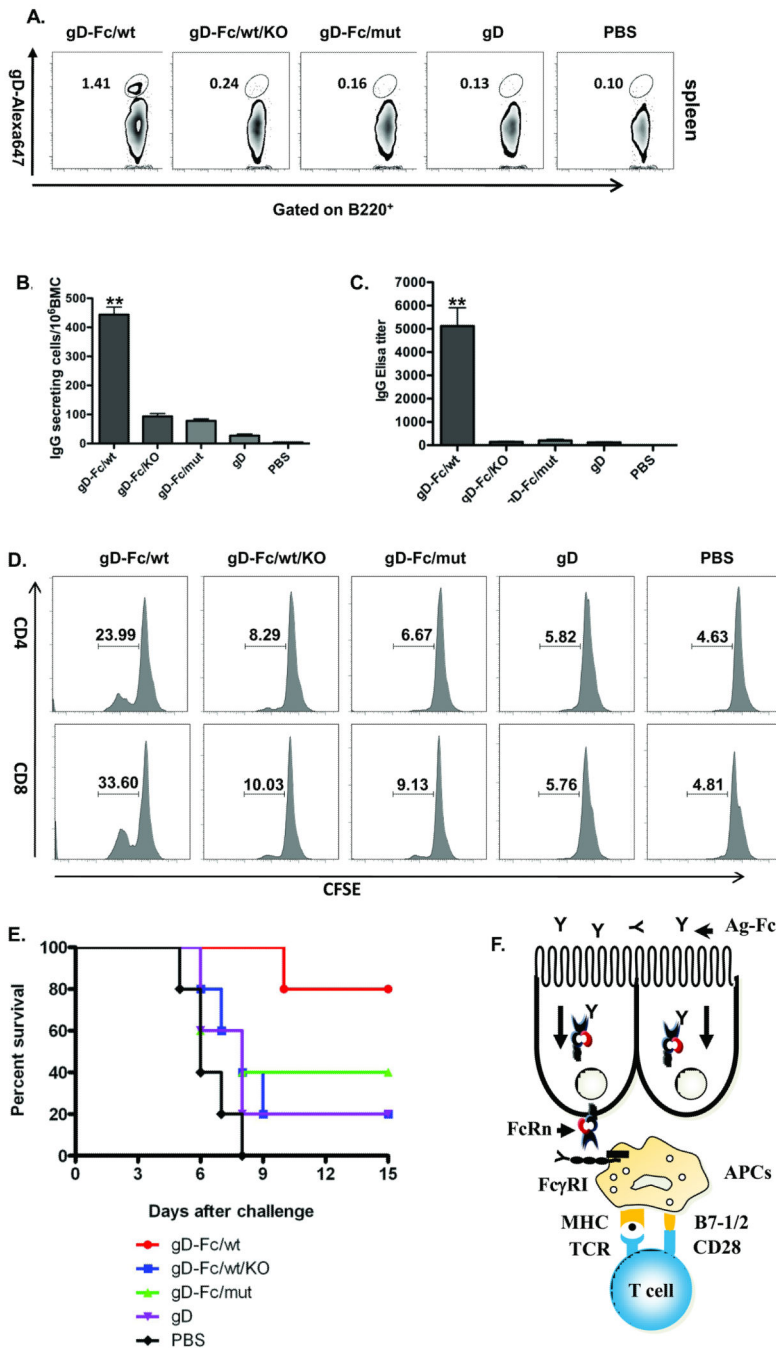


Fig. 4. Increased memory immune response in FcRn-targeted mucosal immunization
(A). Induction of gD specific memory B cells in the spleen. The frequency of gD-specific memory B cells was assessed 6 months after the boost. Memory B cells, defined as B220⁺ gD-surface⁺, were analyzed 6 months after the boost by FACS. Purified gD proteins were labeled with Alexa Fluro647. Spleen cells (2×10^6) were incubated with the 1 μ g Alexa Fluro647-labeled gD proteins and B220 antibody. Numbers in the quadrants are the percentage of gD-specific memory B lymphocytes.

(B). Long-lived HSV gD-specific antibody-secreting cells in the bone marrow. Bone marrow cells removed 6 months after the boost were placed on gD-coated plates and quantified by ELISPOT analysis of IgG-secreting plasma cells. Data were pooled from two separate experiments with five mice in each experiment. The graphs were plotted based on the average ELISPOT for replicate wells. Values marked with asterisk are significantly greater ($P < 0.01$) from the gD-Fc/wt protein-immunized mice than those of other groups as indicated.

(C). Durability of HSV-2 gD-specific serum IgG response. In two separate experiments, HSV-2 gD-specific IgG was quantified by ELISA in serum by endpoint titer from five mice at 6 months after the boost. HSV-specific IgG antibody was not detected in PBS-immunized mice.

(D). Long-lived gD specific T cell memory to FcRn-targeted mucosal vaccination. Spleen cells were isolated from the immunized mice six months after the boost, stained with CFSE, and stimulated *in vitro* with 20 $\mu\text{g/ml}$ of purified gD for 4 days. Data are expressed in CFSE histograms of fluorescence intensity versus the number of fluorescing cells, indicating the percentage of the cell population positive for CD4 and CD8 antigen. Numbers in the quadrants are the percentage of CD4⁺ and CD8⁺ proliferating T cells. Representative flow cytometry profiles of two similar experiments with three mice per group are shown. Immunization conditions are displayed on the top.

(E). Mean survival following genital HSV-2 challenge six months following the boost. The immunized mice were challenged intravaginally with 1×10^4 pfu of HSV-2. Percentage of mice protected on the indicated days is calculated as the number of mice surviving divided by the number of mice in each group ($n=5$).

(F). Proposed model of FcRn-mediated mucosal vaccine delivery. The Fc-fused antigens are transported by FcRn and targeted to the mucosal antigen presenting cells (APCs), such as dendritic cells. Antigen is taken up by pinocytosis or Fc γ RI-mediated endocytosis in APCs, then processed and presented to T cells.